Hydraulic scale modelling of the rating curve for a gauging station with challenging geometry

Øyvind Pedersen, Jochen Aberle and Nils Rüther

ABSTRACT

Direct discharge measurements during flood events can be challenging from a technical as well as from a safety point of view. Therefore, flood discharges are often estimated by extrapolating a rating curve. Extrapolations far outside the range of the directly measured discharges are common, although the associated errors can be large. In this article, a novel method to determine suitable stage measurement locations and derive rating curves using a hydraulic scale model is presented. A hydraulic scale model for a natural gauging station site is produced with a computer numerical control technique, making a detailed representation of the prototype topography and bathymetry. The site is characterized by a complex geometry, and the results of the scale model study reveal that the current location of stage measurement is not suitable for determining the rating curve for high flows. The scale model is used to identify potential locations for future stage measurements, and a flood rating curve is constructed based on field measurements for low flows and scale model data for high flows. The study shows how hydraulic scale modelling can be used to provide more reliable rating curves for large discharges and evaluate new or existing gauging stations located at sites with challenging measurement conditions.

Key words | flood discharge, gauging station, hydraulic modelling, hydraulic scale model, observation uncertainty, rating curve

Øyvind Pedersen (corresponding author)
Nils Rüther
Department of Hydraulic and Environmental Engineering,
Norwegian University of Science and Technology,
Trondheim,
Norway
E-mail: *oyvind.pedersen@ntnu.no*

Jochen Aberle
Leichtweiß-Institut für Wasserbau,
Technische Universität Braunschweig,
Braunschweig,
Germany

INTRODUCTION

Information on flood discharges from gauging stations is important for the determination of return periods of flood events and flood risk assessment. The discharge in rivers is often determined indirectly by measuring the stage (h) and estimating the discharge (Q) from a stage–discharge rating curve. The latter is normally obtained from a series of direct measurements of both discharge and stage for a range of flows. During floods the stage can often be measured with reasonable accuracy, or otherwise be determined by high water marks (WMO 2010) or even from historical data (Engeland *et al.* 2017). The direct measurement of discharge is much more difficult during high flows, as high velocities and stages in the river cause both technical and safety concerns. Catching the peak flow during a flood event can also be logistically challenging, because flood events are inherently rare and often short in duration. Recently, new methods for the continuous measurement of discharges have become available, for example, based on image velocimetry (e.g., Fujita 2017; Legleiter *et al.* 2017). In practice, the discharge is still often estimated by extrapolating the rating curve, although the relationship between the measured stage and the estimated discharge is associated with large uncertainty (e.g., Kuczera 1996; Di Baldassarre & Montanari 2009; Di Baldassarre & Claps 2011; Di Baldassarre *et al.* 2012; Steinbakk *et al.* 2016), which may dominate other sources of error (Domeneghetti *et al.* 2012).

doi: 10.2166/nh.2019.044

A straightforward method for the extrapolation of stage–discharge curves is to simply extend the last segment of the rating function (see Equation (1)) past the measured range of discharges. However, changes in hydraulic control, local energy losses, roughness, section shape or change in hydraulic behaviour of structures may cause such extrapolations to be inaccurate (Lang *et al.* 2010). Many studies have focused on the quantification of extrapolation errors of stage–discharge curves and on the improvement of extrapolation techniques. For example, using power-law functions, Di Baldassarre & Montanari (2009) estimated the average extrapolation error to be 13.8% for a reach in the River Po, Italy. Since mathematical functions used for the extrapolation are usually smooth, the extrapolation of rating curves often leads to systematic under- or overestimation, and the error increases with the increasing deviation from the last gauged discharge (Kuczera 1996; Di Baldassarre *et al.* 2012; Krajewski *et al.* 2018).

A variety of methods exist for the reduction of the error due to extrapolation of rating curves. The slope-conveyance method (WMO 2010) can be used to reduce the extrapolation uncertainty for rating curves with channel control, but is limited to conditions where uniform flow equations are valid. Leonard *et al.* (2000) calibrated a model based on a modified Manning equation against observations at low stages to improve extrapolation. The model used in Leonard *et al.* (2000) requires the measurement of the local energy slope to calibrate the Manning roughness coefficient. Petersen-Øverleir (2006) developed a numerical rating curve model for critical flow from a reservoir based on the energy equations. The models developed by Leonard *et al.* (2000) and Petersen-Øverleir (2006) performed better than classic power-law models at predicting observed flow for stages higher than the calibration data. These methods are, however, restricted in use. The Manning or Chezy equations are based on the assumption of uniform flow although they can be used for evaluating the head loss in gradually varied flow (Chow 1959). The equations derived in Petersen-Øverleir (2006) are restricted to steady critical flows from reservoirs. For unsteady, gradually or rapidly varied, non-uniform flow, one- or two-dimensional numerical models can be applied. For example, Lang *et al.* (2010) used a model based on the Saint-Venant equations to extrapolate rating curves in eight Mediterranean catchments. Domeneghetti *et al.* (2012) demonstrated that a constrained approach for rating-curve construction, where the highest available direct stage–discharge measurement is used to calibrate a quasi two-dimensional numerical model, involves less uncertainty than the traditional power-law approach for extrapolated flows. However, as hydrostatic pressure is assumed, one- and two-dimensional models are valid only if there is no significant vertical acceleration (Novak *et al.* 2010). Finally, numerical solution techniques for the full three-dimensional Navier–Stokes equations are computationally costly, but have become more viable in recent years (Slotnick *et al.* 2014). For example, Reynolds-averaged Navier–Stokes models have recently been applied to model rating curves for spillways and weirs (Zeng *et al.* 2016) and submerged ogee-weirs (Pedersen *et al.* 2018).

This article presents a novel method to determine suitable stage measurement locations and derive stage–discharge curves using hydraulic scale models with detailed representation of the river bathymetry. To the authors' knowledge, the application of a hydraulic scale model to model rating curves for stream gauging is novel. In addition, the novelty of the study lies in the application of a large hydraulic scale model with a detailed bathymetry to a complex bathymetry and flow case. The detailed representation of the river bathymetry is obtained using large-scale CNC-milling, which has recently been applied successfully to hydraulic scale models (Paquier *et al.* 2018).

The presented results are based on a case study of a gauging station located in a mountainous river with complex bathymetry, operated by the Norwegian Water Resources and Energy Directorate (NVE). The gauging station has a well-established rating curve for lower flows but the determination of flood discharges from extrapolation of the rating curve is known to be problematic. In fact, during a flood event in 2011 the measured peak stage at the station was 4.76 m, corresponding to a discharge of 876 m^3/s or 4.4 times the mean annual flood according to an extrapolation of the current operational rating curve. Field observations and modelling in other parts of the river resulted in the hypothesis that this estimate was biased, which was part of the reason for initiating the present study and constructing a scale-model of the gauging site.

The research goals for the case study are two-fold. First, the case study investigates the possibilities of using hydraulic

scale models to analyse the flow and determine the high-flow stage–discharge curve at gauging sites with complex flow and geometry. Second, the hydraulic scale model is used in tandem with a computational fluid dynamics (CFD) model as part of a hybrid modelling approach (Pedersen & Rüther 2016) combining the advantages of hydraulic scale modelling with CFD. The present article focuses on the findings from the hydraulic scale model.

The findings show how hydraulic scale models with detailed bathymetric representation can be used to analyse flow at gauging stations and determine suitable location for stage measurements, and demonstrate how a novel method based on a hydraulic scale model can be used to derive rating curves for complex sites.

The next section describes the gauging station which is the focus of the present article. This chapter is followed by a review of existing methods for the determination of rating curves. The construction of the scale model and the experimental programme are described in the subsequent section, followed by the presentation and discussion of the results.

STUDY AREA AND DATA

Eggafossen case study

The case study which is the focus of this article is the Eggafossen gauging station, located in the River Gaula in central Norway (Figure 1). The gauging station is operated by the Norwegian Water Resources and Energy Directorate (NVE). It was installed in 1941 and contains over 70 years of stage measurement series. The mean discharge (average over the years 1961–1990) corresponds to 17 m^3/s and the mean annual flood to 199 m^3/s. In recent years, the stage has been measured by using pressure loggers with 30-minute resolution and automatic data transfer. The rating curve at the site has been established based on just over 100 direct field measurements of discharge, ranging up to 249 m^3/s. Discharge measurements are typically conducted using acoustic Doppler current profilers (ADCP) or current meters and the discharge is determined by the velocity-area method.

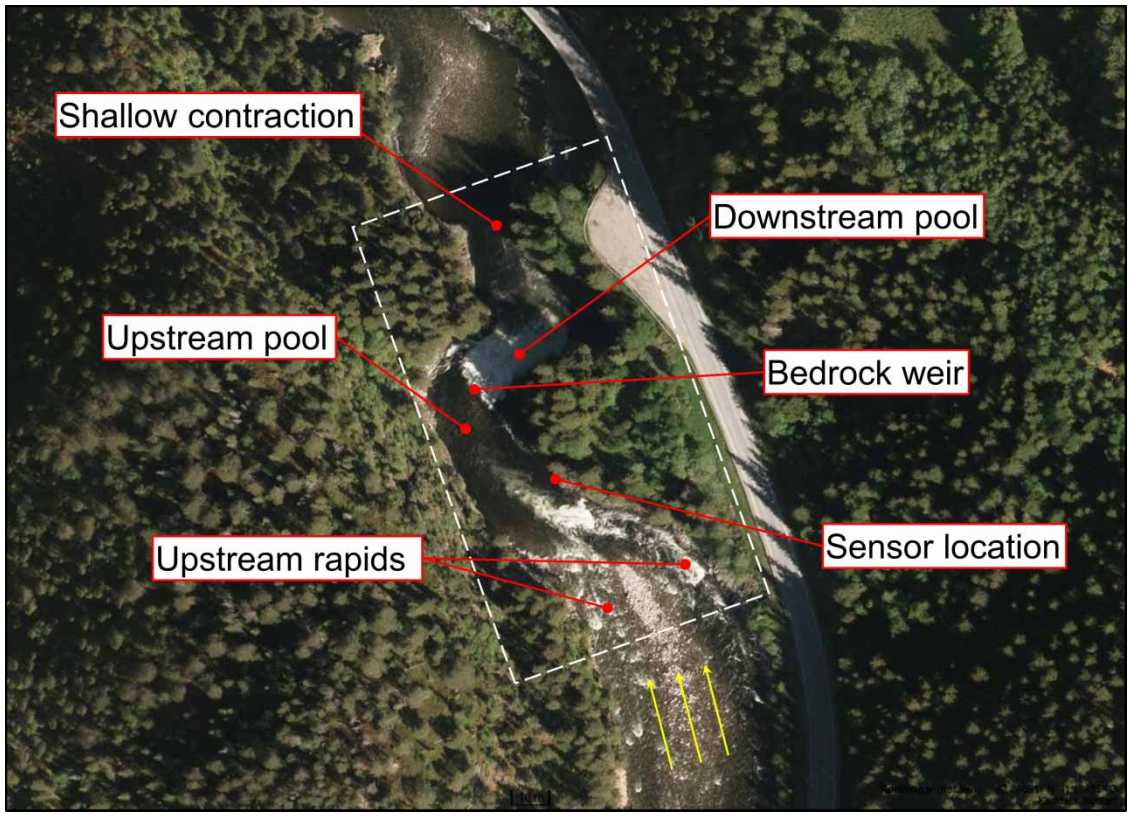

Figure 1 | Orthophotograph of the site. The dashed lines show approximate limits of the scale model described in this article. Photograph: Norwegian Mapping Authority.

Figure 1 shows important features of the study site. The stage is measured by a pressure sensor in a stilling well located in a pool at the right-hand side of the river upstream of a natural bedrock weir. This upstream pool is about 2 m deep at mean discharge. The bedrock weir is a natural ridge, which is perpendicular to the flow and which exerts the flow control for a wide range of discharges. Downstream of the bedrock weir the flow plunges into a deep pool, which has a depth of about 8 m at mean discharge. A contraction defines the outlet from this deep pool and the river flows shallow further downstream. The contraction can cause the water level in the downstream pool to submerge the bedrock weir during large flows leading to partial control. At mean discharge the difference between the upstream and downstream water levels in the pool is approximately 5 m. Upstream of the sensor location, the river is characterized by two rapids, which are separated by a stone bank into two chutes. The rapids are curving leftward and the corresponding bend starts with a smooth curve that gets sharper towards the pool.

Survey

The topographic and bathymetric data used for constructing the scale model were obtained from a survey campaign and from aerial laser scans available from the Norwegian Mapping Authority (these data can be found at www.hoydedata.no). The survey conditions were challenging due to the combination of high velocities in the river and abrupt geometric features in the bedrock. Several techniques were utilized to gather the data. A terrestrial laser scanner was used to scan the terrain above the water surface with a density of approximately 180 points per m^2. Additionally, a total station was used for surveying parts of the terrain and the bathymetry in shallow areas. On average, one point was surveyed per m^2 but a higher point density (2–5 points per m^2) was recorded at breaking points, e.g., the top and foot of the ridge forming the bedrock weir. The upstream and downstream pools were surveyed by sonar from a canoe. The mean density of sonar points was approximately three points per m^2. Due to high velocities, turbulence and air entrainment, it was not possible to obtain bathymetric data in the rapids between the curve and the upstream pool and close to the waterfall in the downstream pool. The geometry in these areas was modelled manually based on visual observations and experiences from the field. Data available from the Norwegian mapping authority were used to complement the measured datasets. All the data were merged to provide a point cloud defining the geometry of the site.

METHODOLOGY

Construction of rating curves for stream gauging

The stage (h) defined as the water surface elevation over a given datum is typically monitored continually at gauging stations. Often, the stage is measured in a stilling well that is hydraulically connected to the river, typically by two or more pressure taps or holes drilled directly in the well. Neglecting the velocity head, the water surface in the stilling well defines the hydraulic head (ψ), which is equal to the stage in the river if the pressure distribution is hydrostatic. Hydrostatic conditions can reasonably be assumed during flows that are normally considered suitable for gauging. However, adverse conditions, for example due to obstructions during floods, can cause vertical accelerations in the flow and hence result in non-hydrostatic pressure conditions.

The critical section or reach determining the stage at the gauging site for a given discharge is often referred to as the station– (Herschy 2009), stage–discharge (WMO 2010) or hydraulic control (e.g., Petersen-Øverleir & Reitan 2009; Le Coz *et al.* 2014). The section or reach controlling the flow can be defined by natural features of the river or an artificial structure. In the case of an artificial structure, such as a flume or a weir, the rating curve can sometimes (but not always) be established from known theoretical or empirical relationships, and only a few control measurements are necessary (WMO 2010). If the hydraulic control is exerted by a relatively uniform channel section (channel control) or a cross section constricting the channel (section control) in a natural river, the rating curve is usually established by discharge measurements for a range of stages. For this purpose, current meters or ADCP are used to measure velocities and flow depths and the discharge is calculated by integrating the discharge over the cross-sectional area

of flow (Herschy 2009); this method is also known as the velocity-area method.

It may further be necessary to distinguish between complete control and compound control (Rantz 1982; WMO 2010). A section or channel reach exerting complete control governs the stage for all discharges. A compound control, on the other hand, exists if two or more sections (or reaches) exert the stage-control for the range of discharges. An example according to WMO (2010) is the case when a section control is drowned out due to backwater effects from a downstream channel or cross section. For such conditions, the flow is controlled by a section-control at low stages and by channel-control or a downstream section-control at higher stages. During the transition between different controls the stage can be influenced by several partial controls.

The combination of paired stage–discharge measurements forms the basis for the construction of the rating curve, which is commonly obtained by fitting one or more power-law functions to the gaugings (Dymond & Christian 1982; Herschy 2009). According to Leopold & Maddock (1953), power-laws of the form $Q = Ch^b$, where C denotes a coefficient in appropriate dimensions and b an exponent, describe the stage–discharge relationship for many hydraulic conditions in natural rivers over a wide range of discharges. According to open-channel hydraulics theory, the exponent b is related to the hydraulic exponent for critical flow or uniform flow, and can be derived or approximated for an arbitrary cross-sectional shape (Chow 1959). For example, b = 3/2 for a rectangular section and 5/2 for a V-shaped section. For uniform flow in a wide rectangular channel, b = 5/3. Empirical values for b for natural channels can also be found in the literature. For example, according to Herschy (2009), b is in practice almost always larger than 2 and often larger than 3 for (critical) section controls in deep, narrow rivers. For wide rivers with channel control, b varies between 1.3 and 1.8 (Herschy 2009).

If the hydraulic control changes with discharge, as outlined above, a single power-law relationship may not be sufficient to describe the full rating curve. To account for this aspect, the rating curve can be divided into several segments based on threshold levels. The power-law segments can be expressed as follows (after Reitan & Petersen-Overleir 2009):

$$\begin{aligned} Q &= 0 && \text{for } h < h_{01} \\ Q &= C_1(h - h_{01})^{b1} && \text{for } h_{01} < h < h_{s1} \\ Q &= C_n(h - h_{0n})^{bn} && \text{for } h_{sn-1} < h < h_{sn} \end{aligned} \quad (1)$$

where h_{01} is the stage of zero flow in the river, h_{0n} is the theoretical stage of zero flow for segment n, h_{si} is the threshold between segment n and $n+1$, C_n is the coefficient for segment n, b_n is the exponent for segment n.

Typically, statistical models are used to determine these parameters and the uncertainty associated with them (Moyeed & Clarke 2005; Reitan & Petersen-Overleir 2008); the likely number of segments and associated thresholds can also be determined (Reitan & Petersen-Overleir 2009).

It is worth keeping in mind that the interpretation of the rating curve parameters becomes challenging for more complex situations such as compound controls or irregular geometries. Moreover, it is important that the values of the parameters are kept within physically reasonable limits to guarantee the validity of the rating curve (Le Coz *et al.* 2014). Guidance on analysis and practical examples for physical interpretation of rating curve parameters can be found in stream gauging literature (Rantz 1982; WMO 2010).

The above considerations apply to cases where data are available for the parameterization of the power-law functions. As mentioned above, this is often not the case for extreme discharges where direct flow-measurements are particularly difficult.

Hydraulic scale modelling method

Model construction

The scale model of the Eggafossen gauging site was constructed using a computer numerical control (CNC) technique in a machining laboratory to make full use of the surveyed data and to achieve a high geometric similarity. The input for the CNC-based milling technique was a stereolithographic (STL) three-dimensional surface model, created by fitting a patchwork of continuous non-uniform rational B-spline (NURBS) surfaces to the point cloud from the survey. The STL model was compared to the original point

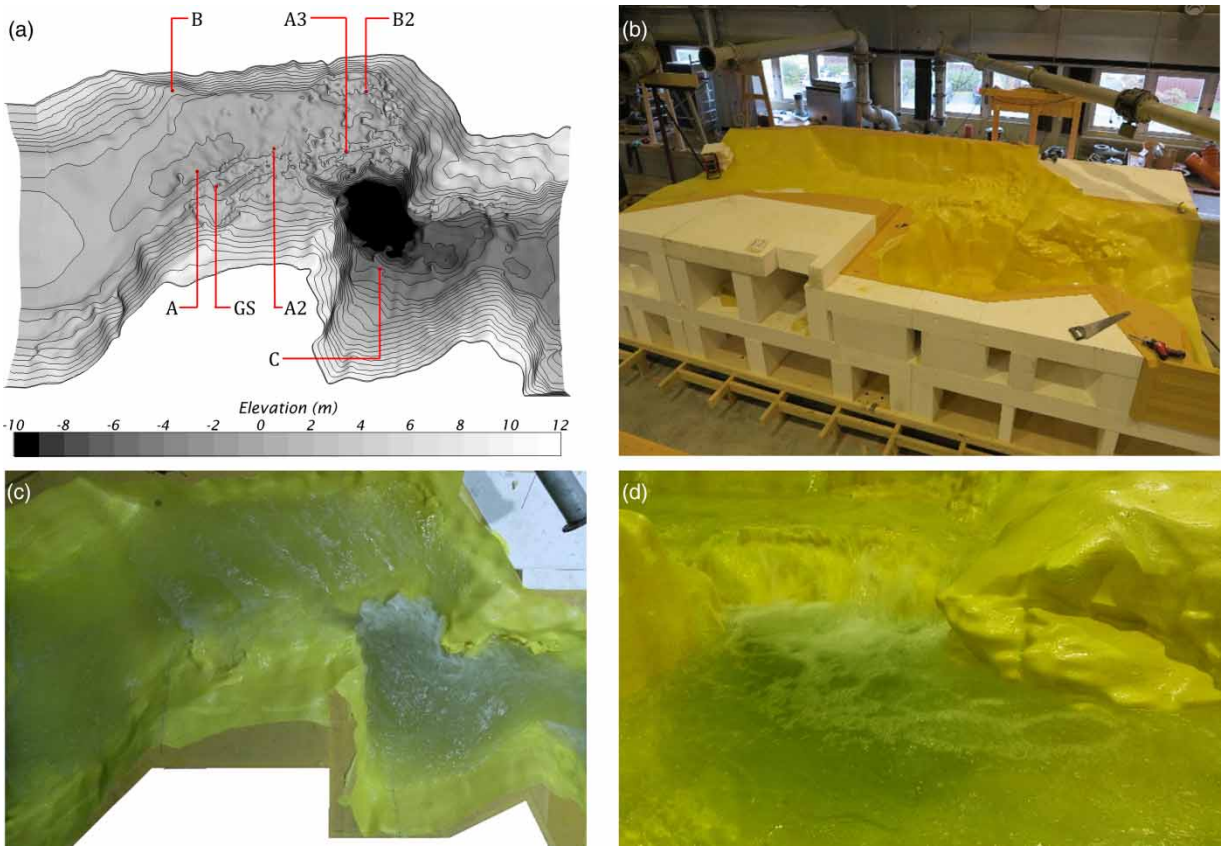

Figure 2 | (a) Geometry for the hydraulic scale model, contour lines are 1 m equidistant; (b) model geometry under construction in the laboratory; (c) bird's-eye view of the scale model with water flowing from left to right; (d) detailed view of the scale model waterfall.

cloud to assess the accuracy of the surface representing the survey data. For a subset of points containing the upstream pool and bedrock weir, 68.7% of the points were within a difference of 0.05 m from the STL model surface. For all the survey points, 70.8% fell within a distance of 0.2 m from the surface. The 29.2% of the points with errors larger than 0.2 m were mainly located in parts of the model where the required accuracy is not high, i.e., areas were the velocity is low and areas that are not submerged, even during extreme conditions.

The model was milled out from a low-density polyvinyl chloride (PVC) foam core material based on the STL model in a geometric scale of 1:17.5. The downstream boundary of the model was downstream of the shallow contraction of the deep pool (see Figure 1) so that the backwater effect from the contraction could be accounted for in the model tests for high discharges. Due to the resulting size of the model (6×4 m), individual parts of the model were milled separately and then assembled in the hydraulic laboratory of the Norwegian University of Science and Technology (see Pedersen & Rüther 2016).

Experimental setup and instrumentation

Two pipes connected to the water circuit of the laboratory delivered up to 0.507 m^3/s to the model corresponding to a maximum prototype discharge of 640 m^3/s. The flow rate was measured by inductive flow meters installed to the pipes and the inflow was delivered vertically to an inlet box, in which the flow was conditioned.

Hydraulic heads in the hydraulic scale model (ψ_{HSM}) were measured by stilling wells connected to pressure taps via plastic hoses in points GS, A, B and C (see Figure 2(a)) using needle gauges (accuracy 0.1 mm). Point gauging

station (GS) corresponds to the location of the existing NVE sensor used for the stage measurements, point A is located along the thalweg of the model, point B is located on the left side of the river, and point C is located in the downstream pool. Note that points GS, A and B define a cross section of the river.

Water surface elevations (h_{HSM}) were measured directly using ultrasonic sensors with operating range 65–600 mm in points A, A2, A3, B, B2 and C (see Figure 2) with a sampling frequency of 60 Hz. Point A2 is located along the thalweg of the model, the water levels above the bedrock weir were measured at point A3 and point B2 is located on the left-hand side of the river. The recorded values were averaged over 5 minutes and the corresponding standard deviations of the time series were in the order of magnitude 10 mm or smaller. We observed that the water surface gradient at point GS was too large at most flows to give good ultrasound readings. Therefore, the water surface elevation was instead measured directly above the pressure intake by using a needle gauge. For the subsequent analysis it should be kept in mind that the mentioned adverse measurement conditions introduced an extra source of error in these recordings (i.e., the water surface elevations at point GS).

Experimental programme

For the hydraulic tests, the flow was Froude-scaled as gravity forces are dominant. The chosen scale resulted in a minimum depth of 5 cm over the bedrock weir so that water tension effects were negligible (e.g., Novak *et al.* 2010). In total, 286 runs were carried out for steady discharges ranging between 7.9 m^3/s and 648.7 m^3/s in prototype scale (0.0062–0.5064 m^3/s in model scale). The measurements with the needle gauges in the stilling wells were carried out twice for each discharge to ensure the stationarity of the water levels. Similarly, the discharge measurements were monitored to ensure constant discharge. Visual observations during the experiments showed that the bedrock weir remained non-submerged for flow rates $Q < \sim 500\ m^3/s$; i.e., the water level at the gauging station was not influenced by the downstream channel constriction for these flow rates. For flow rates $Q > \sim 500\ m^3/s$, the bedrock weir was becoming submerged.

RESULTS AND DISCUSSION

Model validation

The model was validated by a comparison of stage–discharge data from the scale model with available field stage–discharge data. Figure 3 shows the hydraulic heads from the hydraulic scale model experiments and the field measurements measured at point GS (ψ_{HSM}^{GS} and ψ_{DFM}^{GS}, respectively) as a function of discharge in prototype scale. As the largest directly measured field discharge is 249 m^3/s, the figure shows the range $Q < 250\ m^3/s$. The figure shows a good agreement between the measurements for $Q < 100\ m^3/s$. However, for larger discharges the data-series separate and the scatter in the scale model data becomes larger for $Q = \sim 150$–$250\ m^3/s$ with the mean for each discharge being lower than the corresponding stage obtained from the field measurements. This is due to the local hydraulic conditions at point GS during high flows, which will be discussed in more detail in the next section.

In general, scale models should be calibrated against available data from the prototype, if possible. In particular, the model has to be calibrated if the effective friction resistance in the model is different from the prototype. In this case study, the scale model results fit the field data well for $Q < 100\ m^3/s$, which indicates that friction losses along the river bed are negligible. As the geometry of the model was reproduced with high accuracy, it has not been attempted to calibrate the model to get a better fit for $Q > 100\ m^3/s$ since the site (point GS) turned out to be unsuitable for modelling high flows, as will be shown below.

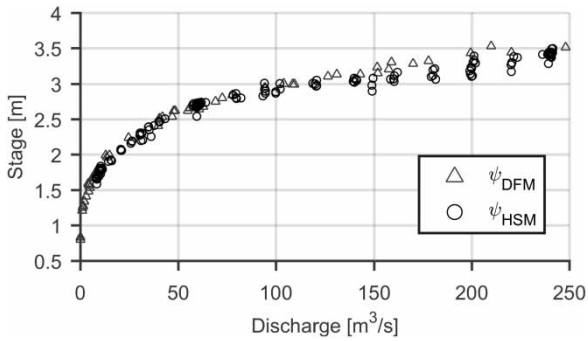

Figure 3 | Comparison between direct field measurements (DFM) and hydraulic scale model (HSM) for hydraulic heads at point GS in the range of directly measured discharges ($Q < 250\ m^3/s$).

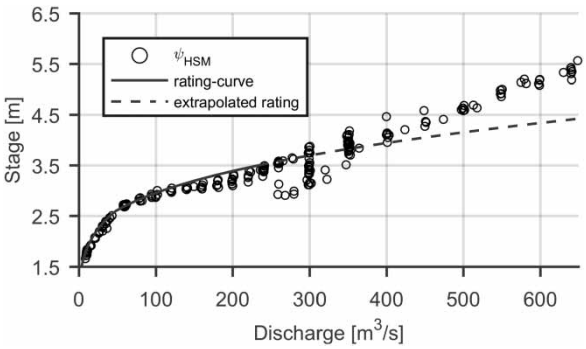

Figure 4 | Comparison between scale model stage–discharge data and current operational rating curve for all discharges.

Rating curve at high flows

Figure 4 shows the operational rating curve as well as 286 measured hydraulic heads from the scale model at point GS for discharges up to 648.7 m^3/s. The operational rating curve has two segments (see Equation (1)) with $C_1 = 4.717$, $h_{01} = 0.592$, $b_1 = 3.308$, and $C_2 = 30.169$, $h_{02} = 1.419$, $b_2 = 2.580$. The threshold between the segments, $h_{s1} = 2.580$. In Figure 4, the second segment of the rating-function has been extended beyond the range of direct field measurements of $Q < 249\ m^3/s$.

The scatter in the scale model data for discharges ranging from $Q = 250$ to $400\ m^3/s$ can be attributed to the local flow conditions at point GS. Figure 5 shows the flow situation in the prototype and the model for a discharge of $Q = 200\ m^3/s$ at point GS (indicated by the arrows), which is the highest flow at which photo observations are available at this point. The figure reveals an obstruction just upstream of point GS causing recirculating flow and a steep transversal gradient between the recirculating zone and the main flow for flows $Q > \sim 200\ m^3/s$. The obstruction clearly disturbs the flow close to the sensor location causing non-hydrostatic pressure conditions. In the scale model tests, the recirculation zone and transversal water surface gradient were observed to be sensitive to relatively small changes in the direction and magnitude of the inflow from the upstream rapids into the upstream pool. This is likely to be the reason for the scatter in the hydraulic head data (ψ_{HSM}^{GS}) of the scale model for the corresponding discharges. As the direction of the flow inflow and magnitude to the upstream pool may be influenced by the leftward bend upstream of the rapids, the sensitivity to inflow conditions will be tested in a follow-up study using a CFD model.

The observations discussed above indicate that the stage measurements at point GS become influenced by the local hydraulic conditions for $Q > 100$–$150\ m^3/s$, and become highly sensitive in the discharge range between 250 and $400\ m^3/s$. This, in turn, increases the uncertainty of the stage measurements and rating curve and it can be concluded that point GS is not suited for modelling the rating curve outside of the gauged range.

Figure 4 reveals that for $Q > 400\ m^3/s$ the scale model results are characterized by a steeper slope of the rating curve than the extrapolated segmented rating curve. Due to both the upstream obstruction and the apparent change in hydraulic control at higher discharges, the scale model

Figure 5 | Flow at $\sim 200\ m^3/s$ in the field (top) and the hydraulic scale model (bottom). The arrows indicate the location of point GS. Flow direction from the top towards the bottom.

results indicate that the operational rating curve may also not be reliable for $Q > 400\ \mathrm{m^3/s}$.

Determining suitable locations for stage measurements at high flows

If pressure conditions are non-hydrostatic, stilling wells are not suitable for stage measurements. Moreover, significant non-hydrostatic pressure conditions are indicative of conditions that will likely mean unstable measurement conditions even if the water surface is measured directly rather than by stilling well. In the scale model, both the stage (h) and hydraulic head (ψ) were measured separately, and may therefore be used to evaluate non-hydrostatic pressures in terms of head by investigating the deviation between ψ and h.

Figure 6 presents ψ and h from the scale model in points GS, A and B for the full discharge range. Up to approximately $Q = 60\ \mathrm{m^3/s}$, the measured hydraulic head at point GS (ψ^{GS}_{HSM}) corresponds well with the measured stage (h^{GS}_{HSM}) (Figure 6(a)). For $Q > 60\ \mathrm{m^3/s}$, h^{GS}_{HSM} is generally lower than ψ^{GS}_{HSM} because of the local hydraulic conditions, and the pressure distribution can no longer be assumed to be hydrostatic.

Figure 6(b) shows that the hydraulic head in point A (ψ^{A}_{HSM}) is also affected by the flow conditions caused by the obstruction. Similar to the data shown in Figure 6(a), the water stage measurements (h^{A}_{HSM}) are in agreement with ψ^{A}_{HSM} up to $60\ \mathrm{m^3/s}$ and deviate for $Q > 60\ \mathrm{m^3/s}$. Visual observations indicated that this is due to a combination of standing waves causing relatively large vertical velocity components at point A and disturbances due to the obstruction at point GS.

Figure 6(c) shows that ψ^{B}_{HSM} is not influenced by the aforementioned obstructions as the water surface elevation measurements h^{B}_{HSM} are in good agreement with ψ^{B}_{HSM} for the range of considered discharges. Note that no data are available at point B for $Q < 50\ \mathrm{m^3/s}$ because this location is not submerged at low discharges.

Figure 6(d) shows the absolute relative difference, $ARD\% = |(\psi - h)/\psi| \times 100\%$, between the measured hydraulic head and the water surface elevation with

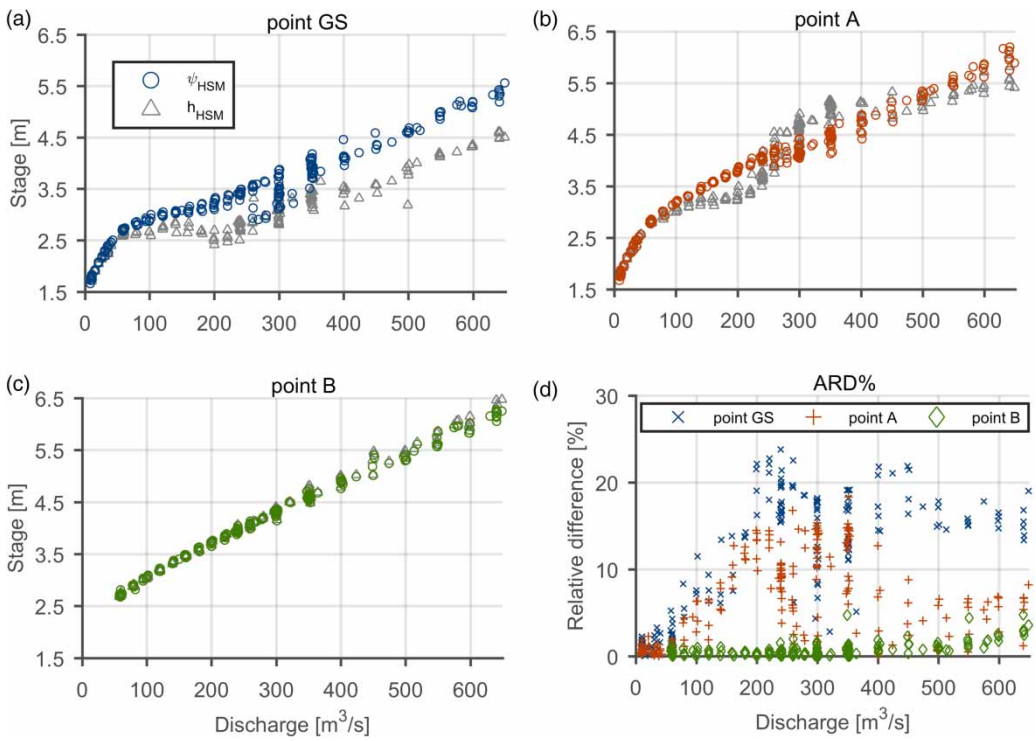

Figure 6 | Measured hydraulic heads and stage from the scale model experiments for (a) points GS, (b) point A, (c) point B and (d) absolute relative difference between hydraulic head and stage.

discharge. From the figure, it can be seen that the difference is smaller than 5% at both point GS and point A for discharges smaller than 60 m^3/s. The deviations rise to approximately 15–25% for larger discharges. On the other hand, the relative difference at point B never exceeds 5% in the evaluated range of discharges. Thus, point B seems more suitable for stage measurements at flows higher than 50 m^3/s all the way to extreme floods of 650 m^3/s.

Construction of a rating curve for large flows

As point B has been identified as the most suitable measurement point in the discussion above, an alternative rating curve for large flows has been constructed for this point. Point B is not submerged in the scale model for $Q <$ 50 m^3/s. However, field stage measurements collected with a pressure sensor on the left side of the river indicate that the water surface is level, and ψ^B is approximately equal to ψ^{GS} for $Q <$ ~100 m^3/s. A combination of field gaugings ($\psi^{GS}_{DFM} <$ 100 m^3/s) and ψ^B_{HSM} points may therefore be used as the basis for constructing the rating curve at point B. A rating curve with three segments was fitted to the data with the help of NVEs VF3 software. The software allows the fitting of the parameters in Equation (1), including the number of segments (n), utilizing a Bayesian framework as described in Reitan & Petersen-Overleir (2009). The resulting parameters are shown in Table 1.

The threshold for the first segment is $h_{s1} = 1.382$ m, corresponding to $Q = 1.5$ m^3/s. The segmentation of the lower part of the curve can be attributed to the requirement that h_0 corresponds to determined point of zero flow. As low flows are not relevant for the problem investigated in this article, this will not be discussed further here. The rating curve and its segmentation can be effectively analysed by using a log-log plot (see e.g., WMO 2010). Plotting ($h - h_{0n}$) as a function of Q on a double logarithmic scale will result in a straight line for each power law segment n, and therefore the data will also fall on a straight line if they adhere to the rating function for segment n. Figure 7 shows a log-log plot for h, ($h - h_{02}$) and ($h - h_{03}$), respectively. Visual inspection of the log-log plots shows that the second segment of the rating curve fits the data well from 5 m^3/s to 100–200 m^3/s, while the third segment fits the data for higher flows, approximately $Q >$ 100 m^3/s. There

Table 1 | Rating-curve parameters found for point B by fitting equation (1) for three segments using the VF3 software. The resulting rating curve is shown in Figure 7

n	1	2	3
C_n	2.199	9.873	111.858
b_n	1.607	2.929	1.247
h_{0n}	0.596	0.857	2.113
h_{sn}	1.382	3.443	–

is no clearly visible point of change in the slope. In fact, the slope is rather characterized by a gradual transition, which indicates a change in hydraulic control due to the effect of partial controls in the intermediate range. The segment threshold between the second and third segment, found by the statistical model, is at $h_{s2} = 3.44$ m corresponding to $Q = 159.6$ m^3/s.

The exponent b_2 for the second segment, valid for discharges between 1.5 m^3/s and 159.6 m^3/s, corresponds to $b_2 = 2.93$. This is a reasonable value for a section control, suggesting a funnel-shaped cross section, i.e., expressing the width as a function of stage, $B(h)^x$, the exponent x is larger than 1. For the third segment, the exponent b_3 is 1.25. This is low for a section control, as theoretically $b =$ 1.5 for a rectangular section and, in practice, values of $b >$ 2 are expected for natural section controls (WMO 2010). Several factors have been identified, which can cause this deviation at high flows:

- head-loss, and consequently backwater effects, are associated with the ~90° bend into the waterfall;
- the curvature of the flow through the pool may cause super-elevation at point B;
- the beginning submergence of the bedrock weir from the downstream pool may start to influence the capacity of the section control.

CONCLUSION

The case study presented in this article demonstrates how a hydraulic scale model can be used to investigate the flow characteristics and stage–discharge relationship at a gauging station site with complex natural hydraulic control. The initial goal of the project was to use scale model data to

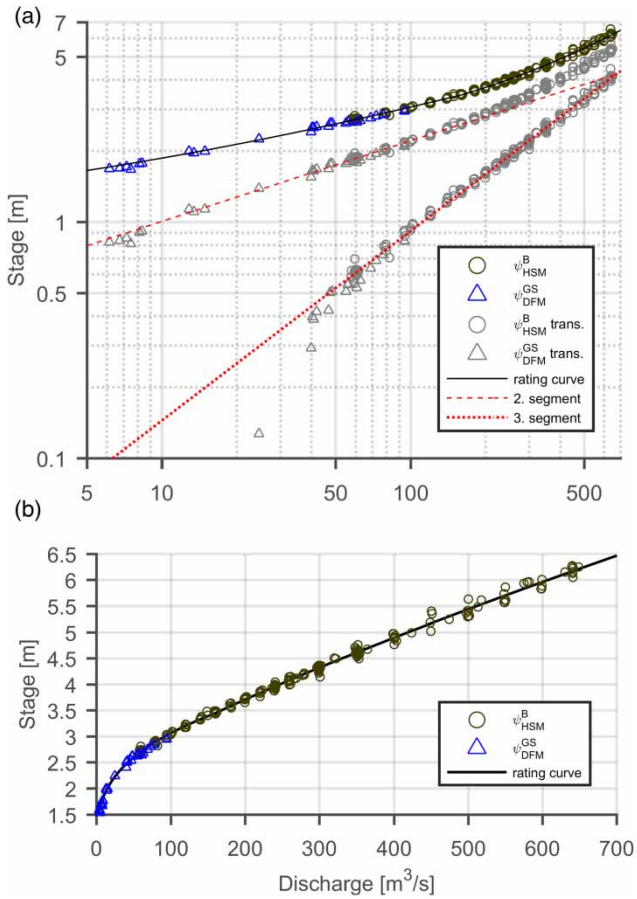

Figure 7 | Multi-segment rating curve fitted to hydraulic scale model and field stage–discharge data: (a) log-log plot, showing the full rating curve and data with stage on the y-axis, as well as the n^{th} rating function and data with translated stage ($h - h_{0n}$) on the y-axis (forming a straight line); (b) standard stage–discharge plot of the rating curve and data.

construct the rating curve for high flows and to gather synthetic data for the extrapolated range of the current rating curve. As demonstrated, the stage measurements were sensitive to local obstruction and it was therefore not possible to model a reasonable rating curve from the scale model experiments at the current GS point. Instead, the hydraulic scale model was used to evaluate the suitability of alternative points of stage measurements for constructing a flood rating curve. The study shows that it is possible to validate a suitable location for stage measurement which does not adhere to the recommendations found in the literature. For example, WMO (2010) gives recommendations for the ideal gauging site, but also recognizes that ideal sites rarely exist in practice. Therefore, the professional judgement of experienced and skilled field hydrologists is always required when choosing the sites of gauging stations. The use of scale models may provide assistance for field hydrologists in choosing suitable locations for stage and discharge measurements and reveal problems with existing gauging stations.

The studied scale modelling method is limited to applications where there are no bed changes at the gauging site. In the current study, the hydraulic control was mainly exerted by a critical flow section, dominated by singular energy losses, and therefore the modelling of friction losses is less important. If the method is to be applied to a channel-type control, the model bed roughness would have to be calibrated. The method also depends on using a relatively large-scale model to avoid scale effects, e.g., surface tension. This will limit the application for gauging stations where the hydraulic control is exerted over a longer river stretch, however this type of gauging station will also likely tend to have less complex geometry.

Based on experience from the current study, the authors suggest that hydraulic scale model studies can be useful for assessing the flow situation at gauging stations and construct synthetic rating curves for existing or planned gauging stations in locations with challenging hydraulic controls.

ACKNOWLEDGEMENTS

The authors would like to acknowledge the Norwegian Research Council and Energy Norway for supporting this study. It is conducted within the project ES519956 'FlomQ – A robust framework to reduce uncertainty in flood prediction'.

REFERENCES

Chow, V. T. 1959 *Open-channel Hydraulics*. McGraw-Hill, New York.

Di Baldassarre, G. & Claps, P. 2011 A hydraulic study on the applicability of flood rating curves. *Hydrology Research* **42** (1), 10–19.

Di Baldassarre, G. & Montanari, A. 2009 Uncertainty in river discharge observations: a quantitative analysis. *Hydrology and Earth System Sciences* **13** (6), 913–921.

Di Baldassarre, G., Laio, F. & Montanari, A. 2012 Effect of observation errors on the uncertainty of design floods.

Physics and Chemistry of the Earth, Parts A/B/C **42–44**, 85–90.

Domeneghetti, A., Castellarin, A. & Brath, A. 2012 Assessing rating-curve uncertainty and its effects on hydraulic model calibration. *Hydrology and Earth System Sciences* **16** (4), 1191–1202.

Dymond, J. R. & Christian, R. 1982 Accuracy of discharge determined from a rating curve. *Hydrological Sciences Journal-Journal Des Sciences Hydrologiques* **27** (4), 493–504.

Engeland, K., Wilson, D., Borsányi, P., Roald, L. & Holmqvist, E. 2017 Use of historical data in flood frequency analysis: a case study for four catchments in Norway. *Hydrology Research* **49** (2), 466–486.

Fujita, I. 2017 Discharge measurements of snowmelt flood by space-time image velocimetry during the night using far-infrared camera. *Water* **9** (4), 269.

Herschy, R. W. 2009 *Streamflow Measurement*, 3rd edn. Taylor & Francis, New York, USA.

Krajewski, A., Banasik, K. & Sikorska, A. E. 2018 Stormflow and suspended sediment routing through a small detention pond with uncertain discharge rating curves. *Hydrology Research* nh2018131.

Kuczera, G. 1996 Correlated rating curve error in flood frequency inference. *Water Resources Research* **32** (7), 2119–2127.

Lang, M., Pobanz, K., Renard, B., Renouf, E. & Sauquet, E. 2010 Extrapolation of rating curves by hydraulic modelling, with application to flood frequency analysis. *Hydrological Sciences Journal-Journal Des Sciences Hydrologiques* **55** (6), 883–898.

Le Coz, J., Renard, B., Bonnifait, L., Branger, F. & Le Boursicaud, R. 2014 Combining hydraulic knowledge and uncertain gaugings in the estimation of hydrometric rating curves: a Bayesian approach. *Journal of Hydrology* **509**, 573–587.

Legleiter, C. J., Kinzel, P. J. & Nelson, J. M. 2017 Remote measurement of river discharge using thermal particle image velocimetry (PIV) and various sources of bathymetric information. *Journal of Hydrology* **554**, 490–506.

Leonard, J., Mietton, M., Najib, H. & Gourbesville, P. 2000 Rating curve modelling with Manning's equation to manage instability and improve extrapolation. *Hydrological Sciences Journal* **45** (5), 739–750.

Leopold, L. B. & Maddock, T. 1953 *The Hydraulic Geometry of Stream Channels and Some Physiographic Implications*. Professional paper, USGS No. 252, US Government Printing Office, Washington, DC, USA.

Moyeed, R. A. & Clarke, R. T. 2005 The use of Bayesian methods for fitting rating curves, with case studies. *Advances in Water Resources* **28** (8), 807–818.

Novak, P., Guinot, V., Jeffrey, A. & Reeve, D. E. 2010 *Hydraulic Modelling – An Introduction*. Spon Press, London, UK.

Paquier, A., Henry, P.-Y., Aberle, J., Navaratnam, C. U., Ruther, N. & Rivière, N. 2018 Hydraulic physical model production with Computer Numerically Controlled (CNC) manufacturing techniques. *E3S Web of Conferences* **40**, 05065.

Pedersen, Ø. & Rüther, N. 2016 Hybrid modeling of a gauging station rating curve. *Procedia Engineering* **154**, 433–440.

Pedersen, Ø., Fleit, G., Pummer, E., Tullis, B. P. & Rüther, N. 2018 Reynolds-averaged Navier-Stokes modeling of submerged ogee weirs. *Journal of Irrigation and Drainage Engineering* **144** (1), 04017059.

Petersen-Øverleir, A. 2006 A robust stage-discharge rating curve model based on critical flow from a reservoir. *Hydrology Research* **37** (3), 217–233.

Petersen-Øverleir, A. & Reitan, T. 2009 Bayesian analysis of stage-fall-discharge models for gauging stations affected by variable backwater. *Hydrological Processes* **23** (21), 3057–3074.

Rantz, S. E. 1982 Measurement and computation of streamflow. Volume 1. Measurement of stage and discharge. Volume 2. Computation of discharge. US Geological Survey Water-Supply Paper 2175.

Reitan, T. & Petersen-Overleir, A. 2008 Bayesian power-law regression with a location parameter, with applications for construction of discharge rating curves. *Stochastic Environmental Research and Risk Assessment* **22** (3), 351–365.

Reitan, T. & Petersen-Overleir, A. 2009 Bayesian methods for estimating multi-segment discharge rating curves. *Stochastic Environmental Research and Risk Assessment* **23** (5), 627–642.

Slotnick, J., Khodadoust, A., Alonso, J., Darmofal, D., Gropp, W., Lurie, E. & Mavriplis, D. 2014 *CFD Vision 2030 Study: A Path to Revolutionary Computational Aerosciences*. N. C. f. A. Information, Hanover, MD, USA.

Steinbakk, G. H., Thorarinsdottir, T. L., Reitan, T., Schlichting, L., Hølleland, S. & Engeland, K. 2016 Propagation of rating curve uncertainty in design flood estimation. *Water Resources Research* **52** (9), 6897–6915.

WMO 2010 *Manual on Stream Gauging, WMO-No. 1044*, Vols I and II. World Meteorological Organization, Geneva, Switzerland.

Zeng, J., Zhang, L., Ansar, M., Damisse, E. & González-Castro, J. 2016 Applications of computational fluid dynamics to flow ratings at prototype spillways and weirs. II: framework for planning, data assessment, and flow rating. *Journal of Irrigation and Drainage Engineering* **143** (1), 04016073.

First received 23 March 2018; accepted in revised form 27 December 2018. Available online 19 February 2019